ЖУРНАЛ СТРУКТУРНОЙ ХИМИИ

2014. Том 55, № 4 *Июль – август* *С. 664 – 670*

UDC 541.67:548.737

DISILINE-DOPED BORON NITRIDE NANOTUBES: A COMPUTATIONAL STUDY

S. Arshadi[1], A.R. Bekhradnia[2,3], E. Mohammadi[1], A. Asghari[1]

[1]*Department of Chemistry, Payame Noor University, PO Box 19395-3697, Tehran, Iran*
E-mail: chemistry_arshadi@yahoo.com
[2]*Pharmaceutical Sciences Research Center, Department of Medicinal Chemistry, Mazandaran University of Medical Sciences, Sari, Iran*
E-mail: reza_bnia@yahoo.com
[3]*Researcher at Department of Chemistry, Gothenburg University, Gothenburg, Sweden*

Received February, 11, 2013

The properties of the electronic structure of the Disiline-doped boron nitride nanotubes (Disiline-BNNTs) are investigated by a density functional theory (DFT) calculation. The structural forms are firstly optimized and the CS tensors calculated. Subsequently, the chemical-shielding isotropic (CS^I) and chemical shielding anisotropic (CS^A) parameters are found. The shielding values of boron (B) and nitrogen (N) atoms were calculated by Gauge-Including Atomic Orbital (GIAO), Continuous Set of Gauge Transformations (CSGT) and Individual Gauges for Atoms in Molecules (IGAIM) methods, using B3LYP/6-311+G*. The B3LYP level of theory with IGAIM was the best method to evaluate the theoretical chemical shifts for studied models. The results reveal a significant effect of Disiline doping on the chemical shielding tensors at the sites of those ^{11}B and ^{15}N nuclei located in the nearest neighborhood of the Disiline-doped ring. Furthermore, the values of dipole moments and HOMO—LUMO gaps change in the Disiline-doped models in comparison with the original pristine model.

K e y w o r d s: DFT, Disiline, GIAO, chemical shielding, IGAIM, isotropic, anisotropic.

Carbon and non-carbon nanotubes have come into special focus of researches and received increasing attention during the past 10 years, due to their unique and fascinating properties and wide potential applications [1—3]. The electronic and structural properties of BNNTs have been investigated by either computational [4, 5] or experimental [6, 7] studies.

BNNTs are a structural analogy to CNTs that instead alternate boron and nitride atoms to replace the carbon atoms in the hexagonal structure.

Although CNTs and BNNTs have similar structures, their properties are quite different. For example, the electronic properties of CNTs are distinctly different from those of BNNTs because of the large ionicity of B—N bonds [8]. Also, BNNTs have a much better resistance to oxidation in high temperature systems than CNTs [9]. In contrast with CNTs, which exhibit metallic or semiconducting behavior depending on the tubular diameter and chirality, BNNTs are viewed as always semiconductors without any dependence on the structural factors [10].

Moreover, the BNNTs are polar materials because of slight positive charges of boron (B) atoms and the trivial negative charges of nitrogen (N) atoms whereas CNTs are non-polar.

The BN nanotubes are also divided into *armchair*, chiral, and zigzag structures. Theoretical studies predicted that BN nanotubes are dominant in the zigzag arrangement and wide band gap semiconductors [11, 12] regardless of the tube diameter and chirality.

Fig. 1. 2D view of the pristine model of zigzag BNNT

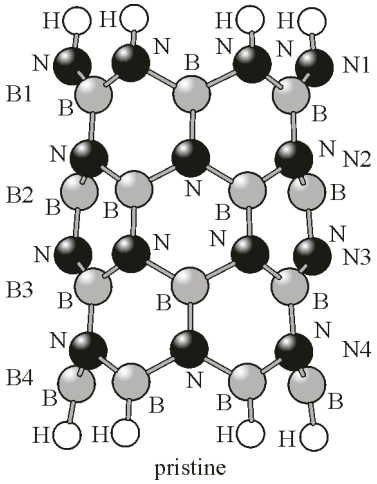

Nuclear magnetic resonance (NMR) spectroscopy is among the most versatile techniques to study the electronic structure properties of materials [13]. Chemical shielding (CS) tensors are very sensitive to the electronic density at the sites of magnetic nuclei, *e.g.* ^{11}B and ^{15}N, and feel changes from any perturbations.

Several methods used with DFT calculations are now available for calculating nuclear shielding. The Gauge-Including Atomic Orbital (GIAO) [14, 15], Individual Gauges for Atoms in Molecules (IGAIM) [16, 17], and Continuous Set of Gauge Transformations (CSGT) [18] methods are three of the most common approaches for calculating nuclear magnetic shielding tensors. In this study, the IGAIM method was employed for studied models. In accordance with these computational results, we wish to extend our future experimental studies as before [19, 20].

COMPUTATIONAL METHODS

In this study, we have considered Pristine and its Disiline-doped models for representative (6,0) zigzag single-walled BNNTs (Figs. 1 and 2).

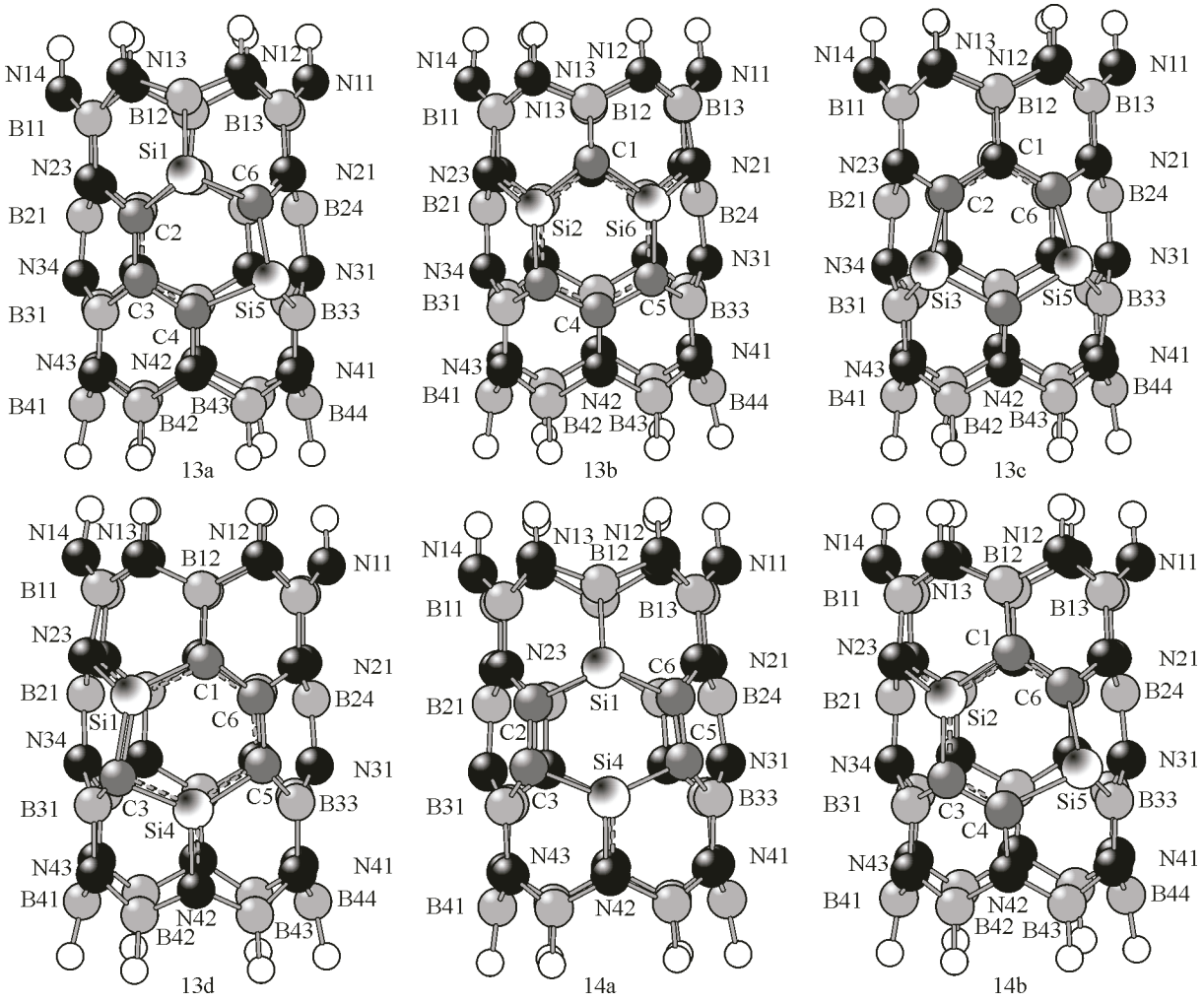

Fig. 2. 2D view of the Disiline-doped models of zigzag BNNT

The pristine model is shown in Fig. 1. It consists of 24 numbers of boron (B) and nitrogen (N) atoms where the two tips of the nanotube are saturated by 12 hydrogen (H) atoms. In pristine zigzag BNNTs, both three boron and nitrogen atoms in the center of the nanotube (Fig. 2) have been replaced by four carbon (C) and two silicon (Si) atoms to construct the six models of Disiline-doped BNNTs (13a, 13b, 13c, 13d, 14a, and 14c).

All calculations were carried out with the Gaussian 98 program package with B3LYP [21] using a hybrid Density Functional Theory (DFT) method for high accuracy results. This method includes a mixture of Hartree-Fock (exact) exchange, Slater local exchange [22], and LYP correlation [23] split-valence 6-311+G* basis set [24, 25].

Firstly, both considered pristine and Disiline-doped representative models of BNNTs were allowed to full relaxation during the geometrical optimization. The geometries were optimized at the B3LYP/6-311+G* level of theory.

To confirm the nature of the stationary species frequency calculations (keyword: FREQ=NORAMAN) were carried out. For minimum state structures, only real frequency values (with a positive sign) have been accepted.

Finally, NMR parameters have been calculated at ^{11}B and ^{15}N nuclei optimized structures.

Chemical shielding tensors (CS^I and CS^A) can be computed with the Continuous Set of Gauge Transformations (CSGT) method and the Gauge-Independent Atomic Orbital (GIAO) method. Magnetic susceptibilities can also be computed with both GIAOs and CGST. GAUSSIAN also supports the IGAIM method (a slight variation on the CSGT method) and the Single Origin method, for both shielding tensor and magnetic susceptibilities. The IGAIM method is the best choice to evaluate the theoretical chemical shifts for the compounds studied.

RESULTS AND DISCUSSION

Geometries. The electronic structure properties of BNNTs were studied using the representative models of (6,0) zigzag BNNTs in which the ends of nanotubes were saturated by hydrogen atoms. Each of the representative models have seven forms (Figs. 1 and 2), namely the pristine model and Disiline-doped models (13a, 13b, 13c, 13d, 14a, and 14b) which have different positions for Si and C atoms.

The calculated structural energies showed a slight difference between the six models of Disiline-doped BNNTs. On the other hand, models 13a—14b were structural isomers.

Furthermore, the most stable structure was for model 13d (–65.63 keV). Also among the values of the HOMO—LUMO gaps of the Disiline-doped models (13a, 13b, 13c, 13d, 14a, and 14c), the largest value was observed for model 13d. Our results indicated that the values of the HOMO—LUMO gaps of the Disiline-doped models were smaller than those for the pristine model. The results are presented in Table 1.

Moreover, a comparison of the dipole moments of models 13a, 13b, 13c, 13d, 14a, and 14b with the pristine model indicated that the dipole moment increased, which means that the contamination modifies substantially the electronic structure of the tube.

T a b l e 1

Energy, LUMO—HOMO *gap*, *dipole moment and electronegativity for pristine and Disiline-doped models of* BNNTs *at the* B3LYP/6-311+G* *level*

Model	Energy, keV	LUMO, eV	HOMO, eV	LUMO—HOMO, eV	Dipole	Electronegativity
Pristine	–52.24	–2.08	–6.86	4.78	6.66	4.47
13a	–65.62	–3.08	–5.71	2.63	7.48	4.39
13b	–65.63	–3.07	–5.22	2.15	8.13	4.14
13c	–65.62	–2.71	–5.40	2.68	7.79	4.06
13d	–65.63	–2.96	–5.96	2.99	7.54	4.46
14a	–65.62	–3.45	–5.14	1.69	7.05	4.30
14b	–65.62	–2.70	–5.20	2.50	8.50	3.95

Table 2

Optimized bond lengths (Å) *and bond angles* (deg.) *for model* 13d *at the* B3LYP/6-311+G* *level*

Bonds	Length	Bonds	Length	Bonds	Length
B12—N12	1.45[1.45]	C1—B12	1.52[1.45]	B13—N12	1.44[1.45]
B12—N13	1.47[1.45]	C6—N21	1.42[1.46]	B24—N31	1.48[1.45]
B13—N21	1.47[1.45]	C5—B33	1.54[1.46]	B43—N41	1.45[1.46]
B24—N21	1.48[1.46]	Si4—N42	1.72[1.45]	B11—N13	1.46[1.45]
B33—N31	1.47[1.46]	C3—B31	1.54[1.46]	B21—N34	1.48[1.45]
B33—N41	1.48[1.45]	Si2—N23	1.72[1.46]	B42—N43	1.46[1.46]
B43—N42	1.46[1.46]	Si2—C1	1.77[1.46]	B11—N14	1.45[1.45]
B42—N42	1.47[1.46]	Si2—C3	1.73[1.45]	B21—N24	1.47[1.46]
B31—N34	1.50[1.46]	C3—Si4	1.76[1.46]	B36—N34	1.47[1.46]
B31—N43	1.48[1.45]	Si4—C5	1.78[1.46]	B41—N44	1.45[1.46]
B11—N23	1.46[1.45]	C5—C6	1.44[1.45]	B24—N26	1.46[1.46]
B21—N23	1.48[1.46]	C6—C1	1.43[1.46]	B34—N31	1.46[1.46]
Bonds	Angle	Bonds	Angle	Bonds	Angle
C1—B12—N12	116[118]	Si4—N42—B43	118[118]	B31—C3—Si2	113[118]
C1—B12—N13	120[118]	C5—B33—N41	124[111]	B31—C3—Si4	104[110]
Si2—N23—B11	115[117]	C5—B33—N31	116[118]	N42—Si4—C3	113[120]
Si2—N23—B21	109[111]	C6—N21—B24	114[111]	N42—Si4—C5	116[120]
C3—B31—N34	121[118]	C6—N21—B13	120[118]	B33—C5—Si4	106[110]
C3—B31—N43	118[120]	C3—Si4—C5	123[118]	B33—C5—C6	121[118]
C1—Si2—C3	124[120]	C5—C6—C1	126[120]	N21—C6—C1	115[118]
Si2—C3—Si4	103[118]	C6—C1—Si2	114[35]	N21—C6—C5	118[120]
Si4—C5—C6	118[118]	N23—Si2—C1	111[118]	B12—C1—Si2	111[118]
Si4—N42—B42	115[118]	N23—Si2—C3	115[120]	B12—C1—C6	122[118]

Tables 2 and 3 present the structural properties consisting of the bond lengths and bond angles for models 13d and 14b (the most stable structure) of zigzag BNNTs. The average B—N bond length in the optimized configuration of pristine BNNT was 1.46 Å, which is consistent with the previously reported DFT calculations.

The deformation of the six-membered ring near the doping site of BNNT was seen by doping the Disiline ring. Also, the changes in the bond angles were more than those in the bond lengths (B—C, C—N, Si—N, B—Si, C—C, and C—Si bonds in addition to B—N) in zigzag Disiline-BNNT.

NMR parameters of (6,0) zigzag BNNTs. The NMR parameters for the investigated models of (6,0) zigzag BNNTs are summarized in Tables 4 and 5. In the pristine model of (6,0) zigzag BNNTs, the NMR parameters are separated into eight layers (Table 4; Fig. 1), which means that the CS parameters for the atoms of each layer have an equivalent chemical environment and electrostatic properties.

Almost no significant difference was observed in the calculated NMR parameters for the atoms of each layer; therefore, just the data for atoms in one layer of the nanotube are presented in Table 4 and also exhibited in Fig. 1.

For B atoms, the atoms located at the edges of the nanotube (B4) have the smallest CS^I value and the largest CS^A one among the other B layers. The CS^I values increased from the edge of the nanotube to the center while CS^A decreased. Different behaviors were viewed for N atoms; layer1 (N1) has the largest CS^I value but the smallest CS^A value among the other N layers. Opposite behaviors were viewed for the changes in CS^I and CS^A values of the other B and N atoms, which were mainly dependent on the lone pair of the N valence shell.

Table 3

Optimized bond lengths (Å) *and bond angles* (deg.) *for model* 14b *at the* B3LYP/6-311+G* *level*

Bonds	Length	Bonds	Length	Bonds	Length
B12—N12	1.44[1.45]	C1—B12	1.53[1.45]	B13—N12	1.46[1.45]
B12—N13	1.46[1.45]	C6—N21	1.42[1.46]	B24—N31	1.46[1.45]
B13—N21	1.48[1.45]	Si5—B33	1.99[1.46]	B43—N41	1.45[1.46]
B24—N21	1.50[1.46]	C4—N42	1.41[1.45]	B11—N13	1.46[1.45]
B33—N31	1.46[1.46]	C3—B31	1.53[1.46]	B21—N34	1.46[1.45]
B33—N41	1.46[1.45]	Si2—N23	1.73[1.46]	B42—N43	1.46[1.46]
B43—N42	1.47[1.46]	Si2—C1	1.76[1.46]	B11—N14	1.45[1.45]
B42—N42	1.47[1.46]	Si2—C3	1.76[1.45]	B21—N24	1.49[1.46]
B31—N34	1.48[1.46]	C3—C4	1.41[1.46]	B36—N34	1.47[1.46]
B31—N43	1.45[1.45]	C4—Si5	1.94[1.46]	B41—N44	1.45[1.46]
B11—N23	1.47[1.45]	Si5—C6	1.90[1.45]	B24—N26	1.46[1.46]
B21—N23	1.49[1.46]	C6—C1	1.40[1.46]	B34—N31	1.47[1.46]
Bonds	Angle	Bonds	Angle	Bonds	Angle
C1—B12—N12	114[118]	C4—N42—B43	122[118]	B31—C3—Si2	115[118]
C1—B12—N13	120[118]	Si5—B33—N41	116[111]	B31—C3—C4	117[110]
Si2—N23—B11	116[117]	si5—B33—N31	122[118]	N42—C4—C3	118[120]
Si2—N23—B21	111[111]	C6—N21—B24	115[111]	N42—C4—si5	117[120]
C3—B31—N34	120[118]	C6—N21—B13	119[118]	B33—si5—C4	86[110]
C3—B31—N43	116[120]	C3—C4—Si5	125[118]	B33—si5—C6	96[118]
C1—Si2—C3	124[120]	Si5—C6—C1	123[120]	N21—C6—C1	116[118]
Si2—C3—C4	117[118]	C6—C1—Si2	107[35]	N21—C6—Si5	120[120]
C4—Si5—C6	101[118]	N23—Si2—C1	111[118]	B12—C1—Si2	114[118]
C4—N42—B42	120[118]	N23—Si2—C3	115[120]	B12—C1—C6	122[118]

In Disiline-doped models (Fig. 2) three B and three N atoms (B22, B23, B32, N22, N23, and N33) in the center of the nanotube were replaced by four carbons atoms and two Si atoms (with different position) to create Disiline-doped BNNTs (Disiline-BNNTs).

The values of the NMR parameters (CS^I and CS^A) of the ^{11}B and ^{15}N atoms in Disiline-doped (6,0) zigzag BNNTs (13a, 13b, 13c, 13d, 14a, and 14b models) are summarized in Table5.

The Table 5 results revealed the significant effect of Disiline doping at the sites of ^{11}B and ^{15}N nuclei located in the nearest neighborhood (nearer distance) of Disiline-doped BNNTs (models 13a, 13b, 13c, 13d, 14a, and 14b).

In the forms (13a, 13b, 13c, 13d, 14a, and 14b) (Fig. 2), which have different positions for C and Si atoms in the corresponding models, the NMR parameters of B12, B31, B33, N21, N23, and N42 were influenced by the direct effects of Disiline doping; hence, their CS tensors detected somechanges due to Disiline doping. Although (N12, N13, N21, N23, N41, N43) and (B11, B13, B21, B24, B31, B42, B43) atoms were not directly bonded, influenced by the Disiline-doped ring, however, due to the sensitivity of the CS tensors, they also underwent some minor changes in the doped model.

Table 4

NMR *parameters of the pristine model*

Nuclei	CS^I	CS^A	Nuclei	CS^I	CS^A
Layer1 (B1)	70.5	44.2	Layer1 (N1)	144.1	90.3
Layer2 (B2)	69.2	39.6	Layer2 (N2)	117.7	180.4
Layer3 (B3)	69.8	42.2	Layer3 (N3)	113.1	189.7
Layer4 (B4)	65.6	56.5	Layer4 (N4)	78.6	234.3

Table 5

NMR *parameters* (ppm) *of doped models of* (6,0) *zigzag* BNNTs

Nuclei	Fig. 13a		Fig. 13b		Fig. 13c		Fig. 13d		Fig. 14a		Fig. 14c	
	CS^I	CS^A	CS^I	CS^A	CS^I	CS^A	CS^I	CS^A	CS^I	CS^A	CS^I	CS^A
B11	69.6	56.5	68.5	42.5	73.0	47.0	70.4	44.3	70.4	44.3	69.3	43.7
B12	43.8	88.3	63.2	57.9	76.3	55.9	66.6	59.0	56.0	83.7	69.2	57.7
B13	71.5	43.2	68.5	42.5	73.0	47.0	71.4	44.3	71.9	30.0	71.6	47.5
B21	72.0	35.0	70.7	34.8	66.0	32.2	68.8	35.5	71.3	39.5	70.2	33.8
B24	72.0	37.1	70.7	34.8	66.0	32.2	68.5	37.7	71.3	39.5	68.1	33.7
B31	72.1	57.7	65.6	57.1	46.3	92.4	65.4	52.4	72.2	54.9	69.0	56.9
B33	41.4	103.9	65.6	57.1	46.3	92.4	68.6	53.7	72.2	54.9	40.8	100.4
B42	72.1	54.1	68.9	54.5	72.6	50.1	66.9	53.3	64.5	55.2	72.1	54.8
B43	67.4	48.2	68.9	54.5	72.6	50.1	68.0	54.8	64.5	55.2	66.8	50.0
N12	116.5	100.2	132.0	88.1	140.2	116.7	130.5	120.4	122.5	99.8	128.5	124.8
N13	112.6	98.1	132.0	88.1	140.1	116.8	144.8	81.1	122.5	99.8	141.2	92.9
N21	10.6	286.2	122.9	156.1	68.9	173.7	82.7	181.6	72.7	222.7	60.0	191.8
N23	64.4	207.2	122.9	156.1	68.9	173.6	116.8	154.0	72.7	222.7	126.2	155.3
N31	97.0	208.0	110.1	189.3	94.5	208.1	108.8	203.1	101.8	220.6	95.4	213.1
N34	106.9	212.7	110.1	189.3	94.6	208.1	107.9	191.1	101.8	220.6	111.9	191.3
N41	74.7	238.3	70.1	254.4	71.3	238.0	68.5	243.9	69.9	251.4	70.9	242.9
N42	37.9	242.9	41.7	234.5	32.4	287.3	97.0	212.6	73.1	214.2	38.0	253.8
N43	74.0	264.3	70.1	254.4	71.0	45.0	62.1	238.0	69.9	251.4	68.5	263.4

CONCLUSIONS

The effect of Disiline doping on the NMR parameters of a single wall BN nanotube was investigated using DFT calculations.

The results indicated that B and N atoms in the pristine model are divided into eight layers, and the calculated changes of ^{11}B and ^{15}N NMR parameters between the layers are presented.

The calculated CS^I and CS^A parameters of the nuclei in each layer are also the same. The B4 atom has the smallest CS^I and the largest CS^A value (^{11}B) among the other boron nuclei, whereas the N1 atom has the largest CS^I and the smallest CS^A value (^{15}N) among the other nitrogen nuclei.

In the Disiline-doped model, the NMR parameters of B and N atoms directly bonded to C and Si atoms significantly changed. The calculated optimization indicated that the most stable structure was for model 13d. The dipole moment of the pristine system considerably changed as Disiline was doped to BNNT. Also the B—N bond lengths and bond angles show changes in the Disiline-doped models.

Acknowledgments. The authors gratefully acknowledge the financial support for this work received from the Mazandaran University of Medical Sciences ″Sabbatical Funds″ and Payame Noor University.

REFERENCES

1. *Loiseau A., Willaime F., Demoncy N., Schramcheko N., Hug G., Colliex C., Pascard H.* // Carbon. – 1998. – **36**. – P. 743.
2. *Chen X., Ma J., Hu Z., Wu Q., Chen Y.* // J. Amer. Chem. Soc. – 2005. – **127**. – P. 17144.
3. *Zhang D., Zhang R.Q.* // Chem. Phys. Lett. – 2003. – **371**. – P. 426.
4. *Nirmala V., Kolandaivel P.* // J. Mol. Struct. (THEOCHEM). – 2007. – **817**. – P. 137.
5. *Mirzaei M. ei al.* // Z. Phys. Chem. – 2009. – **223**. – P. 815.
6. *Oku T.* // Physica B. – 2002. – **323**. – P. 357.
7. *Arenal R., Ferrari A.C., Reich S., Wirtz L., Mevellec J.-Y., Lefrant S., Rubio A., Loiseau A.* // Nano Lett. – 2006. – **6**. – P. 1812.

8. *Chopra N.G., Zettl A.* // Solid State Commun. – 1998. – **105**. – P. 297.
9. *Moon W.H., Hwang H.J.* // Nanotechnology. – 2004. – **15**. – P. 431.
10. *Zhang S.L.* // Phys. Lett. A. – 2001. – **285**. – P. 207.
11. *Guo G., Lin J.* // Phys. Rev. B. – 2005. – **71**. – P. 165402 – 165411.
12. *Blase X., Rubio A., Louie S., Cohen M.* // Europhys. Lett. – 1994. – **28**. – P. 335.
13. *Bovey F.A.* Nuclear magnetic resonance spectroscopy. – San Diego: Academic Press, 1998.
14. *Ditchfield R.* // Mol. Phys. – 1974. – **27**. – P. 789 – 807.
15. *Rohling C.M., Allen L.C., Ditchfield R.* // Chem. Phys. – 1984. – **87**. – P. 9 – 15.
16. *Keith T.A., Bader R.F.W.* // Chem. Phys. Lett. – 1992. – **94**. – P. 1 – 8.
17. *Casanovas J., Namba A.M., Leon S., Aquino G.B.L., da Silva G.V.J., Aleman C.* // J. Org. Chem. – 2001. – **66**. – P. 3775 – 3782.
18. *Keith T.A., Bader R.F.W.* // Chem. Phys. Lett. – 1993. – **210**. – P. 223 – 231.
19. *Kassaee M.Z., Bekhradnia A.R., Arshadi S.* // Asian J. Chem. – 2008. – **20**. – P. 43 – 47.
20. *Kassaee M.Z., Bekhradnia A.R.* // J. Biosci. Bioeng. – 2003. – **95**. – P. 526 – 529.
21. *Frisch M.J. et al.* Gaussian 98; Gaussian: Pittsburgh, PA, 1998.
22. *Becke A.D.* // Phys. Rev. A. – 1988. – **38**. – P. 3098 – 3100.
23. *Lee C., Yang W., Parr R.G.* // Phys. Rev. B. – 1988. – **37**. – P. 785 – 789.
24. a) *Bekhradnia A.R., Arshadi S., Ebrahimnejad A.* // Canad. J. Chem. – 2011. – **89**. – P. 1403 – 1409; b) *Bekhradnia A.R., Arshadi S.* // Monatsh. Chem. – 2007. – **138**. – P. 725 – 734.
25. *Bekhradnia A.R., Arshadi S., Ahmadi S., Karami A.R., Pourbeyram S.* // Chin. J. Chem. – 2011. – **29**. – P. 1347 – 1352.